


ORIGINAL ARTICLE

Open Access



# 3D visualization of hurricane storm surge impact on urban infrastructure

Xinyue Ye<sup>1,2,3\*</sup> , Shoujia Li<sup>1</sup>, Ge Gao<sup>3</sup>, David Retchless<sup>4</sup>, Zhenhang Cai<sup>1</sup>, Galen Newman<sup>1</sup>, Jiaxin Du<sup>1</sup> and Nick Duffield<sup>5</sup>

## Abstract

As climate change intensifies, resulting in more severe rainfall events, coastal cities globally are witnessing significant life and property losses. A growingly crucial component for flood prevention and relief are urban storm flood simulations, which aid in informed decision-making for emergency management. The vastness of data and the intricacies of 3D computations can make visualizing the urban flood effects on infrastructure daunting. This study offers a 3D visualization of the repercussions of hurricane storm surge flooding on Galveston, TX residences, illustrating the impact on each structure and road across varied storm conditions. We employ target detection to pinpoint house door locations, using door inundation as a metric to gauge potential flood damage. Within a GIS-based framework, we model the damage scope for residences exposed to varying storm intensities. Our research achieves three core goals: 1) Estimating the storm inundation levels on homes across different storm conditions; 2) Assessing first-floor elevations to categorize housing damages into three distinct groups; and 3) Through visualization, showcasing the efficacy of a proposed dike designed to shield Galveston Island from future storm surge and flood events.

**Keywords** 3D visualization, Urban flooding, First-floor elevation, Street view images, Digital twin

## 1 Introduction

Urban flooding, particularly from storms and hurricanes, is increasingly causing property damage, social disruption, and exacerbating inequality (Romali et al., 2018). The uptick in extreme rainfall events, a direct consequence of global climate change, has notably impacted many larger cities. This has resulted in considerable damage to urban residents, both in terms of life and property.

These challenges significantly hinder the effective management and evolution of smart cities.

Urban flood simulations play a crucial role in flood prevention and mitigation (Mignot et al., 2019). The advent of smart cities has facilitated a richer, real-time data influx and enhanced technical support for urban flood simulations. However, visualizing the repercussions of urban flooding on infrastructure and buildings remains a formidable challenge, primarily due to the volume and sheer amount of data now available as well as intricate 3D computational needs and options for modeling (Cai et al., 2023; Ye et al., 2023).

While there have been notable advancements in the intricacy and quality of urban flood simulations in recent years, the transition from rudimentary 1D or 2D models to more refined numerical methodologies still has significant gaps. For instance, Zhang et al. (2016) developed a 3D flood model using high-resolution terrain data and a multi-scale unstructured mesh. Although this model provides more detailed information on the flood propagation

\*Correspondence:

Xinyue Ye  
xinyue.ye@tamu.edu

<sup>1</sup> Department of Landscape Architecture & Urban Planning, Texas A&M University, College Station, TX, USA

<sup>2</sup> Department of Computer Science & Engineering, Texas A&M University, College Station, TX, USA

<sup>3</sup> Center for Geospatial Sciences, Applications and Technology, Texas A&M University, College Station, TX, USA

<sup>4</sup> Department of Marine and Coastal Environmental Science, Texas A&M University, Galveston, TX, USA

<sup>5</sup> Department of Electrical and Computer Engineering, Texas A&M University, College Station, TX, USA

process, it lacks specific insights into how floods can impact different types of buildings and urban infrastructure. Further, the computational demands of this method restrict its use to larger spatial scales.

De Santis et al. (2019) extended the urban flood-mapping concept into a three-dimensional virtual environment, enhancing the communication of probable hazard impacts. However, their method's dependence on terrestrial laser scanning is resource-intensive and difficult to scale up for larger urban areas. Additionally, the integration of this technology with existing urban planning and disaster response systems remains unclear. Similarly, Lee et al. (2019) utilized Unreal Engine for interactive 3D visualization. While visually impressive, the use of high-end gaming engines requires significant computational resources and technical expertise, raising questions about scalability and adaptability to different urban contexts or flood scales. High-resolution digital elevation models (DEMs) have provided detailed urban descriptions (Ozdemir et al., 2013), yet they often fail to capture the complexities of urban flooding, especially under extreme future conditions (Neal et al., 2009).

Given these gaps, our research aims to answer the following critical question: "how can 3D visualization effectively represent the implications of flooding on individual structures and roadways under diverse scenarios?" To address this, we use Galveston, TX as a pilot study. This location was chosen for three reasons: (1) as sea levels rise, many coastal cities are expected to face flood management challenges similar to those already faced by Galveston (which is highly vulnerable to storm surge flooding); (2) because construction of a storm surge barrier has already been approved for Galveston, our methods can be tested under both current infrastructure and the planned protective barrier, illustrating their potential broader utility for cost benefit analyses for other locations and coastal protections; and (3) because Galveston's buildings and residences have highly variable first-floor building elevations, the study area selection provides a challenging test case for our damage estimation method.

Galveston has been vulnerable to flooding, hurricanes, and storm surges for centuries due to its flat topography and adjacency to the Gulf of Mexico (Cai et al., 2023). For instance, it has experienced dramatic flood damage from 36.37 billion in Hurricane Ike (2008) to 132.73 billion US dollars in Hurricane Harvey (2017) (DCMCPartners, 2022). To address Galveston's increasingly severe and frequent flooding, scholars proposed the \$31 billion "Ike Dike" (Merrell et al., 2011), which was approved by U.S. House in 2022 (Douglas, 2022); however, limited publications have quantified the effectiveness of Ike Dike in multiple storm scenarios. Moreover, in terms of the city's infrastructure complexity, Galveston's buildings have

non-standardized first-floor elevations since many of them were constructed before Federal Emergency Management Agency (FEMA) Base Flood Elevation (BFE) regulations. This indicates that they are elevated above the ground at different heights (Needham & McIntyre, 2018). Thus, our approach stands out as novel in several key aspects:

1. Targeted Damage Assessment: We incorporate a target detection approach, pinpointing the positions of building entrances. This allows for a more precise and practical assessment of flood impact on individual structures.
2. Door Flooding as a Damage Indicator: Using door flooding as a damage indicator, we simulate potential harm to residences under varied storm conditions. This provides a more relatable and understandable measure of flood impact for urban residents and planners.
3. GIS Framework Integration: Our method operates within a GIS framework, ensuring compatibility with existing urban planning tools and facilitating easier integration into current disaster response systems.

By focusing on these specific, yet practical, aspects of flood impact, we offer an actionable tool for urban planners and emergency responders, enhancing both preparedness and response strategies. A key innovation is the fusion of widely accessible visualization tools from ArcGIS Pro with a novel FFE estimation approach and high-resolution flood scenarios. In our Galveston-based case study, we focus on (1) estimating the extent of storm inundation homes might endure under various storm events; (2) calculating the first-floor elevation to gauge potential structural damages, subsequently categorizing the severity of damage; and (3) employing visualization techniques to demonstrate the proposed dike's efficacy in safeguarding Galveston Island against floods.

## 2 Relevant work

### 2.1 Building damage estimation in flooding events

Flood damage to buildings is typically classified by type or scale. To assess the negative impacts caused by flooding events, Smith and Ward (1998) introduced three criteria to categorize the types of flood damage, including (1) direct vs indirect, or if the damage occurred immediately after the event related to humans and properties; (2) tangible vs intangible, or if the damage can be assessed in monetary values; and (3) primary vs secondary, or if the damage was from the event itself or secondary effects occurred due to flooding, i.e. property loss due to flooding vs services disruption (Smith & Ward, 1998). Based on the combination of the three

criteria, the most representative factors in examining direct-tangible-primary flood damage were found to be building and infrastructure damages (Romali et al., 2018). Other than categorizing the flood damage by type, Merz et al. (2010) utilized spatial scale for means of classification, with categories such as (1) micro-scale which assessed single exposed elements such as individual buildings, (2) meso-scale which assessed spatial aggregations such as land use type, and (3) macro-scale which assessed larger-scale spatial units such as national or international level factors. Among all scales of flood damage assessments, the micro-scaled building analysis demonstrates the most accuracy and requires more research attention (Merz et al., 2010; Romali et al., 2018).

Direct-tangible-primary flood damage at the micro scale is most frequently assessed based on flood depth data and flood damage function curves. According to the synthesized findings on flood damage assessment from Romali et al. (2018), 20 out of 25 reviewed studies used the flood damage function curve as their major flood damage estimation model. Flood depth is the most used parameter in the flood damage function curve (Romali et al., 2018), since its significance is sufficient enough in flood damage estimation without other factors (Chang et al., 2008; Notaro et al., 2014). The flood damage function curve was first proposed by Gilbert White in 1945, initially known as the stage-damage curve or the losses functions, and aimed to predict flood damage in buildings by flood depth (or stage) (Smith, 1994). Its first major application was in the National Flood Insurance Act in the US in 1968, to evaluate the market values of individual homes (Smith, 1994). In 1977, Penning-Rowsell and Chatterton improved the accuracy of original stage-damage curve by calibrating it with existing databases and conducting surveys among valuers and loss adjusters (Smith, 1994).

However, the assumption behind the stage-damage curve that similar buildings would behave similarly in similar situations, has been challenged by subsequent research. These challenges have included how to categorize buildings into more detailed groups for more accurate damage estimation, how to define building values in the calculation (i.e. market value before or after flood events, with or without repair cost), and how to ensure the availability of real data across all study areas (Marvi, 2020). As such, some scholars have proposed ‘what-if analyses’ to predict the potential flood damage on buildings rather than relying on real database and analytical models to simulate water-infrastructure interactions. Further, the use of the fragility function instead of the damage function to capture

the uncertainty of building damage in flood events has also been preferred (Marvi, 2020).

To obtain more accurate flood damage at building scale, recent studies demonstrate several solutions regarding building classification, model validation, and interoperability. For instance, Schinke et al. (2016) modified the assumption by grouping buildings by their construction period (i.e. historic to end Georgian era, early and middle Victorian era, and post war period), and urban structure types (i.e. terraced house, semi-detached house, and detached house) in Heywood, Greater Manchester, UK). Zabret et al. (2018), on the other hand, only considered the general type of house (one-story without basement in Croatia) as building structure input, but they validated their stage-depth curve by using the most recent flooding event (Zabret et al., 2018). Moreover, Martínez-Gomariz et al. (2021) used building entrances to calculate the difference between water inside and outside of a structure, which is a core indicator of the permeable coefficient in identifying building vulnerability in flooding events (Martínez-Gomariz et al., 2021).

Therefore, in “direct-tangible-primary” flood damage estimation, this research contributes to the micro-scale assessment by identifying the inundation depth of individual buildings. In predicting potential flood damage on buildings, we use the entrance of building, its first-floor elevation (FFE), as the indicator for each building rather than grouping buildings by other criteria. Unlike other approaches that have used building entrances and FFE to estimate damages based on field surveys, existing records, or expert knowledge (e.g., Martínez-Gomariz et al., 2021), we demonstrate the feasibility of estimating FFE directly using widely accessible data (i.e., Google street view imagery and NOAA DEM) and open source software (i.e., YOLO-v5) in an urban environment where buildings have highly variable, non-standardized first-floor elevations.

## 2.2 Urban elements and flooding three-dimension visualization

With rapid urbanization and technology development, scholars have increasingly proposed using 3D cadaster and three-dimensional (3D) models to process traditional two-dimensional (2D) urban information for quicker land management and planning policy decisions (Shojaei et al., 2013; Souza & Bueno, 2022). Also, when comparing 2D and 3D spatial data presentation, Dübel et al. (2014) found that 3D spatial data is more effective for approximate navigation and relative positioning with higher visual attraction, while 2D format is more suitable for precise measurement and interpretation with condensed information (Dübel et al., 2014). Given the advantages of 3D spatial data in urban planning, 3D city models have

gained popularity in environmental simulation and decision support; their purposes can be divided into two groups: non-visualization and visualization (Biljecki et al., 2015). Specifically, Biljecki et al. (2015) identified 29 representative 3D city models worldwide by 2015, and 5 of them were designed for non-visualization purposes (i.e. estimation of the solar irradiation, energy demand estimation, aiding positioning), while 24 of them were for visualization purposes, such as geo-visualization, visibility analysis, routing, and flood simulation. Moreover, according to the findings from the latest systematic and bibliometric review on this topic, we have experienced a boom of 3D city models since 2019. Most case studies have occurred in Asian and European cities and most researchers are more interested in the above-ground infrastructure other than below-ground and their connections in urban settings (Souza & Bueno, 2022). Thus, 3D city models in American cities have great potential, especially for visualization purposes.

For the application of 3D models for urban flood management, there are four main components: (1) data processing, (2) urban elements construction, (3) flooding inundation models, and (4) tools for interactivity (Aditya et al., 2011; Gallegos et al., 2009; Marcy et al., 2011). In data processing, the quality (resolution) of the spatial data plays a role in determining model accuracy, since the Digital Elevation Model (DEM) and the Digital Terrain Model (DTM) are two important data sources for 3D infrastructure and flood inundation visualization. Most recent scholars agree that DEMs and DTMs derived from LiDAR point clouds have better horizontal resolution compared to the products derived from other sources (Poulter & Halpin, 2008; Sanders, 2007). In urban elements construction, for city-scale building 3D visualization, most studies use Geographic Markup Language (GML) to obtain Level of Details (LoD2) city information, which refers to a more detailed representation of a building or component, such as terrain, building footprint, and building height. For the specific-use buildings or urban infrastructure, researchers generate LoD3 buildings in SketchUp, 3D's Max, and Rhino to add textures and detailed structures (Buyukdemircioglu & Kocaman, 2020). For flood inundation models, most studies prefer hydrological models for accurate flood depth and extent but in 2D visualization (Gallegos et al., 2009; Gallien et al., 2018; Poulter & Halpin, 2008), while limited studies also use game engines such as Unreal, and Unity for 3D visualization of storms, hurricanes, and extreme flooding effects (Reyes & Chen, 2017). Specific to flood simulation via hydrological models, those simulation models can be categorized by dimensionality, ranging from zero-dimension models with only water level vs flow rate curving, 1D models, such as HEC-RAS code, 2D models using

shallow-water equations, such as MIKE FLOOD, BreZo and Delft3D, and 3D models using Navier-Stoke equations including ADCIRC, FVCOM, and SWAN (Gallien et al., 2018; Sanders, 2007). As for tools for user-interactivity, Marcy et al. (2011) shared new mapping tools for visualization and scenario planning developed from community workshops organized by USGS and NOAA in 2009. These use ESRI's ArcServer and Adobe's FLEX technology to (1) display potential future SLR, (2) map confidence and probability and (3) predict marsh migration and social and economic vulnerability due to SLR (Marcy et al., 2011). Buyukdemircioglu and Kocaman (2020), on the other hand, demonstrated how to integrate 3D city models in virtual reality (VR) platforms, and invited users to wear VR equipment to explore Sahinbey Municipality, Gaziantep, Turkey.

Thus, for 3D visualization of our urban flood model, we use a DEM or DTM derived from LiDAR as the data source to maintain model accuracy. Despite relying on similar, LiDAR-derived data sources, our approach differs from the above-described prior work on visualization of flooding for high resolution, 3D city models in several important ways: 1) We focus on an American, rather than Asian or European, city; 2) We describe a 3D visualization approach that uses widely accessible visualization tools from ArcGIS Pro, rather than specialized gaming engines that are less familiar to city managers and planners who manage flood risk; and 3) we use a highly detailed ADCIRC 3D flood model to explore changes in building-level flood depth and damage across multiple storm scenarios. In so doing, we bridge the gap between water depth accuracy and visual effects in visualizing urban flood inundation.

### 3 Data and methodology

The 3D visualization of urban flooding in Galveston shows each houses' damage levels by simulating the occurrence of storms in 3D space. We evaluate what kind of storm inundation that houses in Galveston can resist. As noted, we categorize the storms into scenarios including 10/100/500-year storm events and a storm like Hurricane Ike. We ran these scenarios with or without a proposed dike in place to protect the city and assessed these scenarios with a 2.4 ft SLR. We calculated the FFE of the houses and considered the case of flood depth crossing FFE as the house being damaged. In the following text, we describe the detailed steps of building this animation (Fig. 1).

#### 3.1 First-floor elevation

House FFE is an important factor in flood mitigation governance and is used in our study to evaluate whether Galveston residences have been damaged and to what extent.



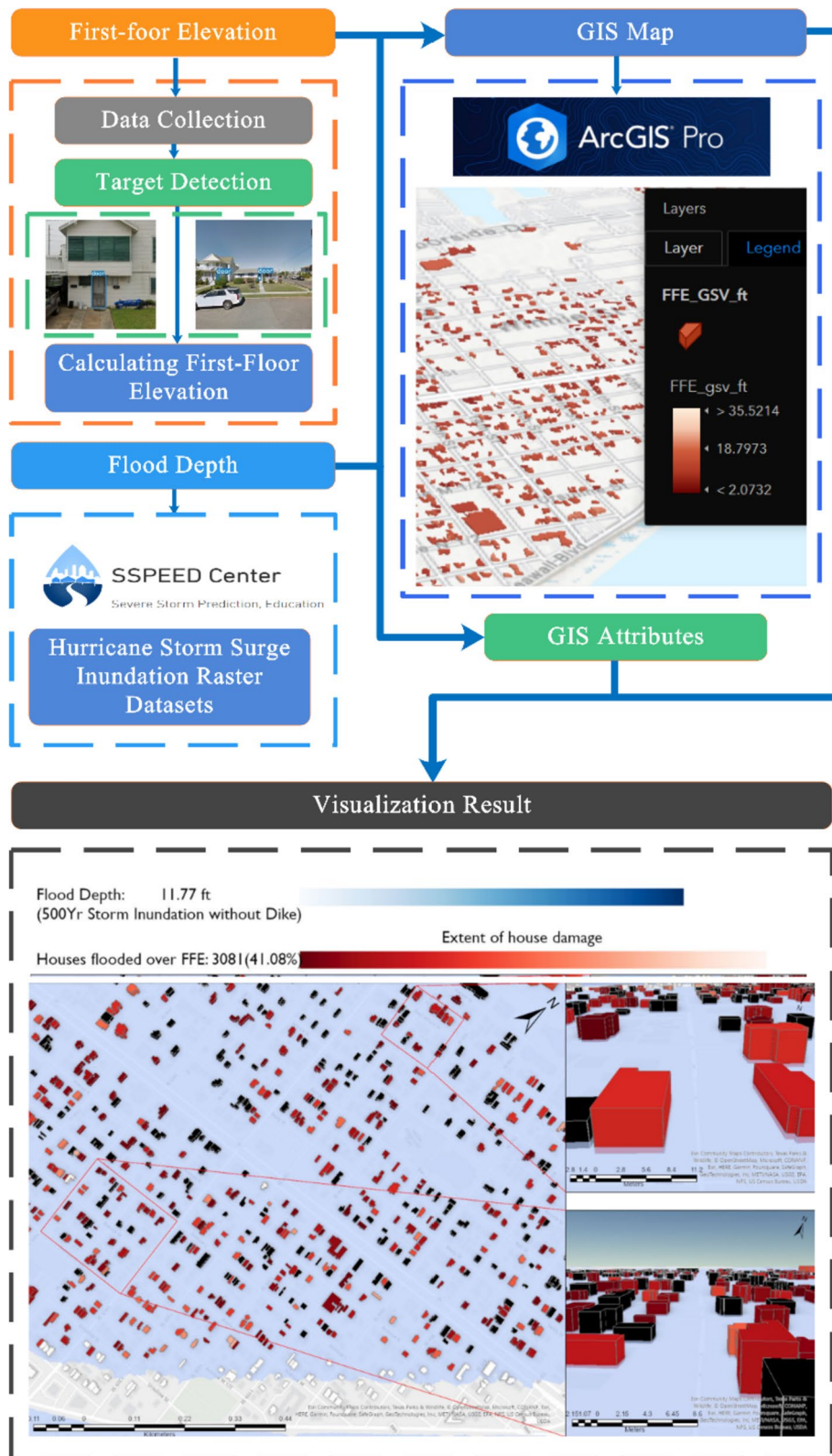


Fig. 1 The steps of visualization

We assess building FFE using the vertical dimension of Google Street View (GSV). Unlike traditional field surveys that rely on manual measurements, our GSV-based measurements use computer vision technology that is capable of processing enormous amounts of data.

### 3.1.1 Data collection

Firstly, we collected the building footprints of all the houses in Galveston, which contain the latitude and longitude of each building's location. The coordinates are the basis to download the street view images (SVIs) from Google Maps as well as the depth maps corresponding with each SVI. Considering the generalizability of our research, the initial data of the proposed workflow can either start from the building footprints or a single list of addresses of the target area (Diaz et al., 2022). For instance, the dataset of Galveston used for accuracy validation only contains addresses but not the coordinate position as the major label for data. When building datasets for further estimation through addresses, the latitude and longitude of these address names are first obtained through a specific Representational State Transfer Application Program Interface (REST API) of geographic map information network services such as Geocoding API provided by the Google Map Platform. From the combined data of addresses with latitude and longitude, we further acquired the SVIs of each house's location.

Upon user-specification of latitude and longitude information, the Street View Service offered by Google Maps searches for photographs within a 50-m radius and provides panoramic images, where available. By defining the latitude and longitude coordinates of each dwelling in the research region, we can acquire SVI images. Each photograph also has time information. We can retrieve static SVI images in any direction, at any angle, and for any point where SVI is available by defining URL parameters given via a typical HTTP request. In our research, field of view (FoV), which determines the horizontal field view of the image, is set to 30° to guarantee the entire front face of the target house is captured, as shown in Fig. 2.

We also downloaded the DEM data for the case study area, which was obtained from the NOAA Sea Level Rise Observatory (derived from LiDAR data). The DEM dataset, which is referenced to the North American Vertical Datum of 1988 (NAVD88, Geoid12B) with vertical measurements in meters, a horizontal resolution of 1 m, and in accordance with the North American Datum of 1983 (NAD83) in the horizontal dimension, extensively covers Brazoria, Chambers, Galveston, Harris, and Liberty Counties in Texas. The DEM serves as the basis for providing the elevation of the shooting point and the ground level of the building, so that both are in the same elevation coordinate system. FFE refers to elevation and not

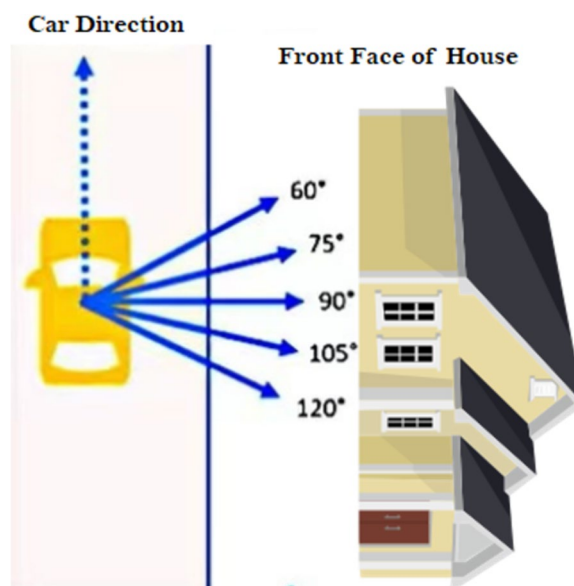


**Fig. 2** The demonstration of SVI collection

height, which does not refer to the height of the first floor to the ground, so the DEM provides us with a level surface. We perform our calculations on this data. We give a more detailed description of the usage of DEM in the subsequent calculation methods.

### 3.1.2 Target detection

For door detection, we adopted the YOLO-v5 (You Only Look Once-v5) model composed of three primary components: a backbone generating picture features at various granularities; a mixing and combining these diverse characteristics; and a head consuming this combined data to predict boxes and classes, which is one of the most widely used models in target detection; this is depicted in Fig. 3.

The YOLO-v5 model is able to detect objects with great speed and accuracy due to the fact that it transmits each batch via the data loader (Wu et al., 2021) and incorporates cross stage partial network (CSPNet) (Wang et al., 2020) into Darknet as the backbone for feature extraction from SVIs in the case study. In addition to the above-mentioned design characteristics, YOLO-v5 employs a number of data augmentation techniques that benefit our workflow, such as mosaic data enhancement (which enriches the data by tiling separate SVIs in varying proportions) and random cropping (which increases tolerance for occlusion since doors are occasionally obscured by fences, decorations, and other objects). While the wrong detections can still occur, Fig. 4 shows examples of detected and missing doors using model trained in Ning et al. (2022)'s work. The primary causes of problems

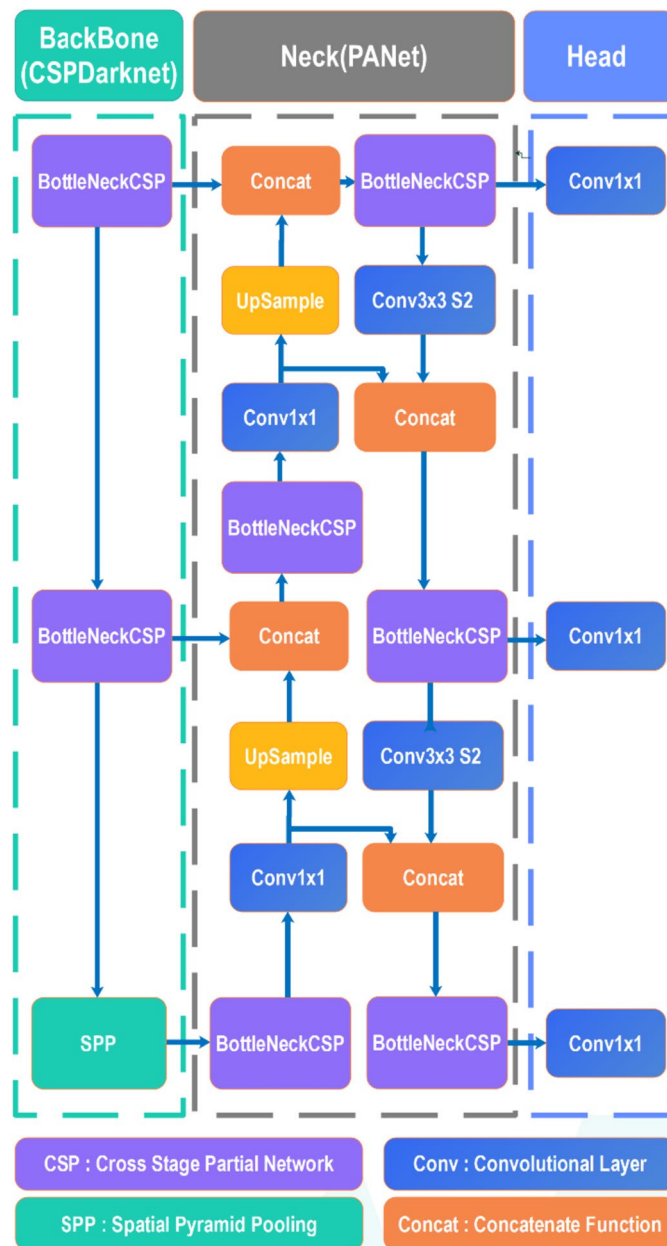


**Fig. 3** The architecture of YOLO-v5 model

leading to incorrect and missing detections include imperfect training models, door occlusion, and issues with angles.

Since the old version of the model classified various kinds of objects in the street view and is likely to make wrong detections, in order to improve model compatibility and prevent some targets from being undetectable or misclassified, we selected images under special circumstances (such as SVIs whose doors are blocked

by various types of plants, pillars, decorations and SVIs) which are relatively blurry due to the data source, and then added them to the training set to enrich its diversity, part of the special cases is shown in Fig. 5.

We adopt Ning et al. (2022)'s training procedure but extended the training dataset from 490 to 1,134 GSVs, with 908 images used as the training set, and 226 images used as the testing set. A RTX 2070 SUPER NVIDIA GPU is used to train YOLO-v5 for 100 epochs



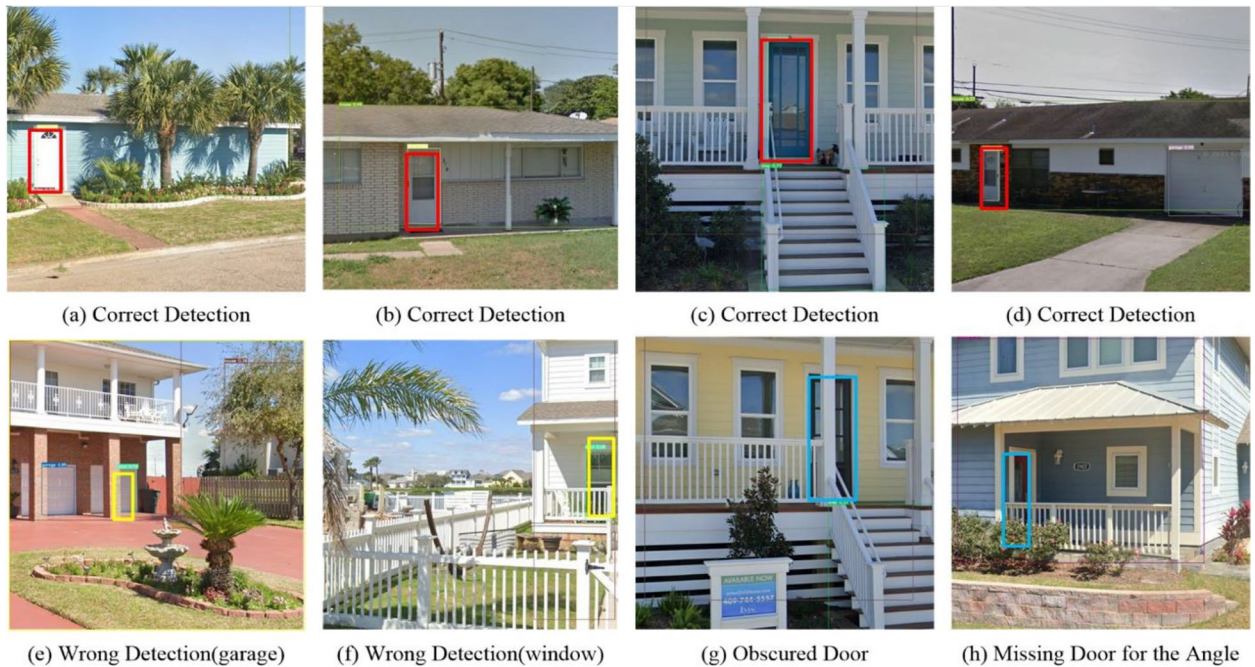


**Fig. 4** The correct, wrong, and missing detections of the old model



**Fig. 5** The part of the special cases added into new training set

with batch size set to 16 and the number of learnable parameters set to large. The results of partial test cases are shown in Fig. 6.

To achieve the best detection result, the argument of object confidence threshold is set to 0.25. In addition, the argument representing the Intersection over Union (IOU)



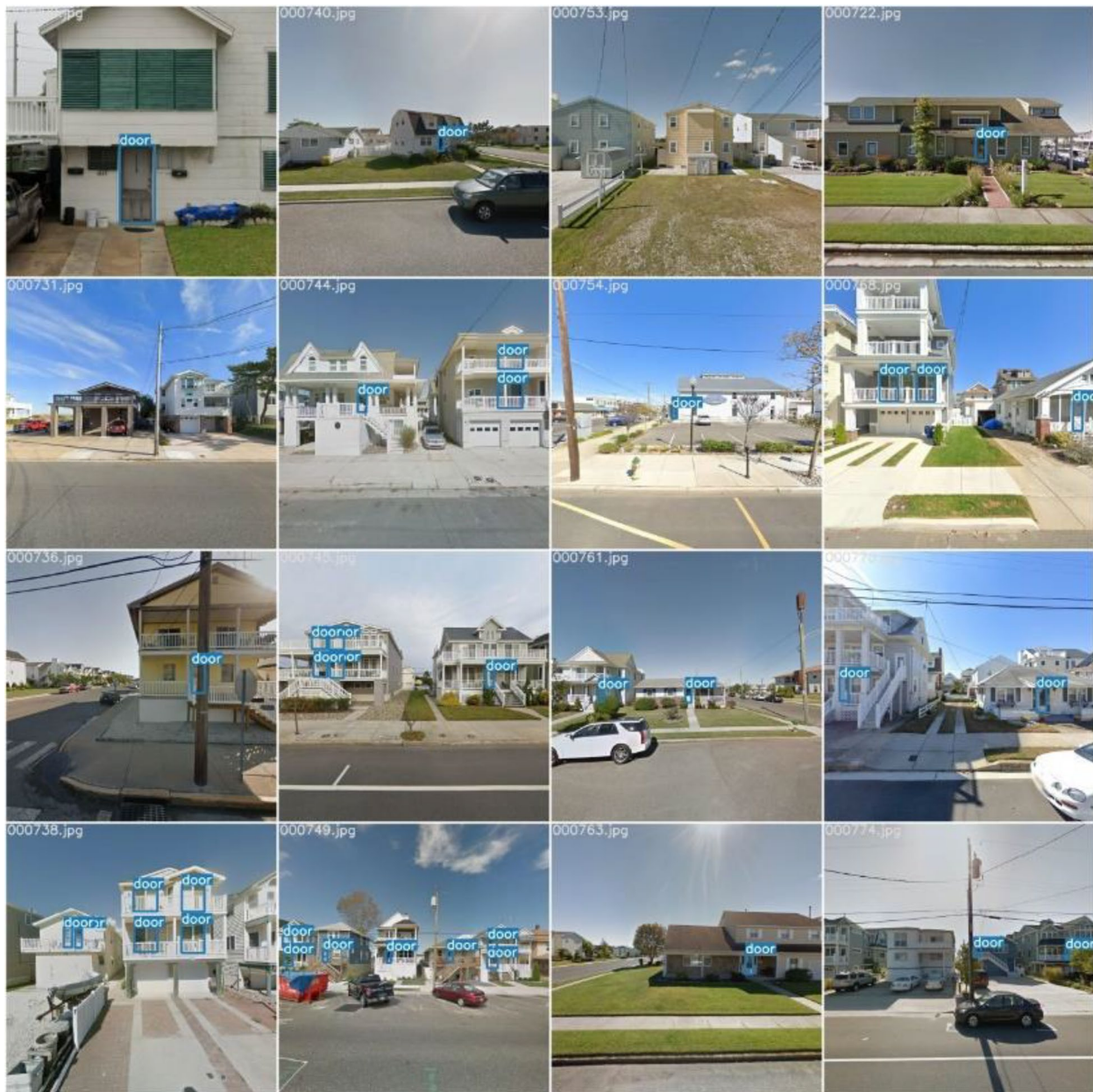


**Fig. 6** The results of partial test cases

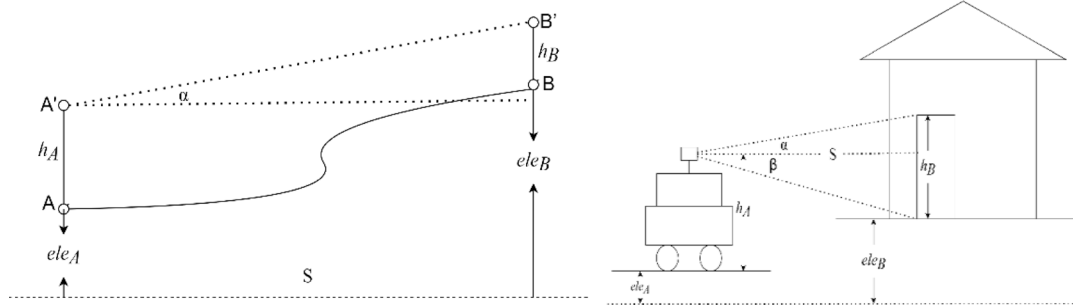
threshold for Non-Maximum Suppression (NMS) is set to 0.45, indicating that the rectangular boxes of the two detection results are kept if the overlapping portion is less than 0.45. Otherwise, the two rectangular boxes should constitute a single detection result, with only one of them being retained.

**3.1.3 Calculating first-floor elevation**

As shown in Fig. 7, according to the principle of triangulation, if we consider  $ele_B$  as the FFE we want to calculate, it is shown as Eq. (1):

$$ele_B = Stan\alpha + h_A + ele_A - h_B \tag{1}$$

Thus,  $ele_A$  means the elevation of shooting point (derived from the DEM data) and  $h_A$  is the height of the shooting point (derived from the depth map). In the study, point A refers to the car point where the street view was taken. For  $\alpha$  and  $\beta$ , it is the altitude angles from the camera center of the street view car to the top and bottom point of the target house’s door. Meanwhile,  $h_B$  is the door height, which we take to be uniformly 2.02 m. However, there is a difference between the calculation of



**(a)The principle of triangulation**

**(b)The principal of calculating FFE**

**Fig. 7** Comparison of triangulation and calculating FFE

FFE and triangulation, in that we do not use the horizontal distance, *S*, but use  $\alpha$  and  $\beta$ . The formula for *Stana* is shown as Eq. (2):

$$Stan\alpha = \frac{h_B \sin\alpha * \cos\beta}{\sin(\alpha + \beta)} \tag{2}$$

So, the equality of FFE is shown as Eq. (3):

$$ele_B = h_A + ele_A - \frac{h_B \sin\beta * \cos\alpha}{\sin(\alpha + \beta)} \tag{3}$$

**3.1.4 Map result to building footprints**

We originally obtained building footprints for 20,317 houses in Galveston. 130,272 GSVs and 16,464 depth maps and panoramas were obtained based on these building footprints. After calculating FFE for all the houses in Galveston, the results were remapped from the point coordinates to the building footprints, because the buildings were used as the unit of analysis. We successfully calculated the FFE of 13,465 buildings in Galveston. Following the elimination of unavailable outcomes, including incorrect detections, missing data, and other similar instances, a total of 8,897 viable results remained. Then, when remapping the results into the maps, some points did not correspond with any footprints due to transform errors. In the end, we modeled the FFE for 7584 houses after eliminating the outcomes with outdated GSVs, which is around 40% of the total houses in Galveston.

**3.2 Flood depth**

Storm magnitude is another important parameter which impacts housing damage. Therefore, we used the hurricane storm surge inundation raster datasets from the Rice University SSPEED Center (<https://www.sspeerd.rice.edu/>).

This dataset includes 16 storm scenarios: 10/100/500-year storms and a storm similar to Hurricane Ike. We also consider the protection of the proposed Ike Dike and 2.4ft SLR added to each storm scenario. Table 1 shows the results simulated by ADCIRC (Advanced Circulation) modeling. The 2.4 ft SLR estimate was chosen because it is consistent with the rate of Galveston shoreline retreat rate after 1930 (Historical Shoreline Changes in Trinity, Galveston, West, and East Bays, Texas Gulf Coast, 1986) and is also the most likely late century (2080) SLR amount for Galveston under an intermediate scenario projection from the US Army Corps of Engineers (USACE) and US National Oceanic and Atmospheric Administration (NOAA) SLR (see USACE Coastal Texas Protection and Restoration Feasibility Study Final Feasibility Report, Appendix D – Annex 1, p. 47, [https://www.swg.usace.army.mil/Portals/26/CTX\\_MR\\_AppendixD\\_Annex1%20%28ERDC%20Spine%20Morphology%29\\_1.pdf](https://www.swg.usace.army.mil/Portals/26/CTX_MR_AppendixD_Annex1%20%28ERDC%20Spine%20Morphology%29_1.pdf)).

Based on the flood depth simulated data across all storm scenarios, both the proposed Ike Dike and 2.4ft SLR would influence the Galveston flood depth significantly. With the Ike Dike, the flood depth would decrease ~11.8% (~13.7% with SLR) across all scenarios on average; With a 2.4 ft SLR, the flood depth would

**Table 1** Flood depth (ft)

	10-Year Storm	Hurricane Ike	100-Year Storm	500-Year Storm
Base	2.36	6.39	7.71	11.77
Dike	2.05	3.81	3.97	5.10
SLR-Base	3.58	8.67	11.25	14.20
SLR-Dike	2.76	3.48	4.83	6.03



increase ~8.4% across all base scenarios on average, and ~3.6% across all dike scenarios on average.

### 4 Results

We visualized the outcome in the ArcGIS Pro environment and added DEM data as the elevation base to display the results along with the terrain. First, we linked the building footprint data with the FFE data into a singular scene layer. Then, we created a new layer to simulate different levels of flood depth, which had the same area as Galveston; the height is displayed by absolute height. The damage to each house can be viewed by increasing the

flood height. The state of the houses varies for different flood depths, and we classify the state of the houses into three types: completely undamaged, damaged, and inundated, where inundated is defined as flooded at or above the FEE level. We use three colors to represent the states of property damage, orange - completely undamaged, red - damaged, and black - inundated as Fig. 8 shows. We summed up the number of inundated houses for each classification for display, and also calculated their percentage. We then exported the resulting maps corresponding to the 16 storm scenarios and placed them in order of severity to make the final animation. In this

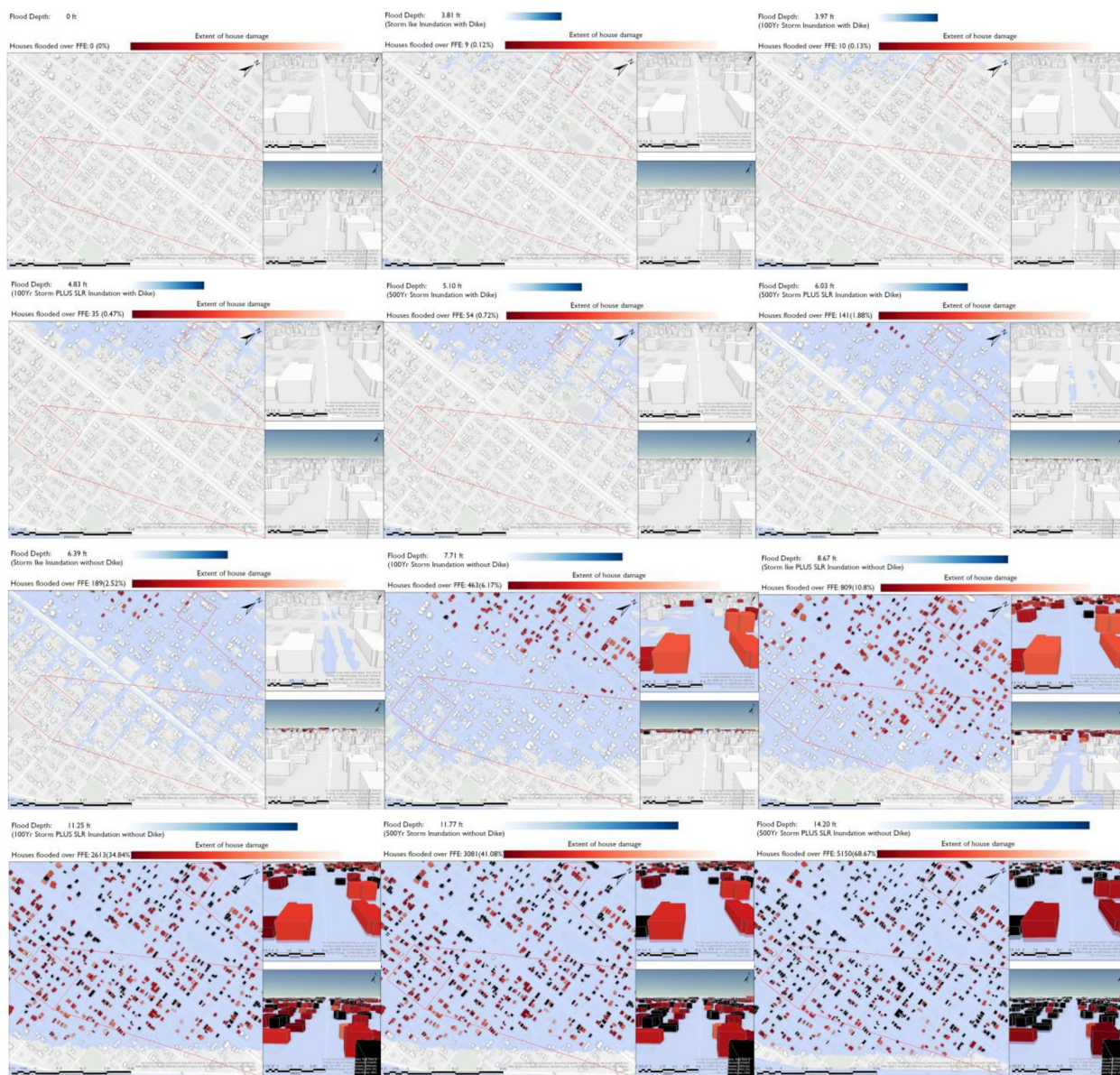


Fig. 8 The visualization of flooding in Galveston



section, we describe this animation process in detail and how it shows how each flood affects each house. Figure 8 shows our final animation.

The flood visualization output shows the number and extent of damaged houses under each different storm scenario, which is illustrated in Fig. 8. A completely undamaged house means that there is no water on the ground currently, and it is a white house in the animation. Damaged houses mean that there is water on the ground, but not more than the FFE (shown in varying degrees of red), with the darker red representing the more severe damage. A flooded house means that the flood depth has exceeded the FFE and is shown as a black house. In addition, there are also three maps with different orientations (top, north and south views) to show more comprehensive information.

## 5 Discussion

With the mounting global concerns of rising sea levels and increasingly regular flash floods, our research results are crucial. They highlight that when a storm engulfs the island, flooding primarily originates from the northwest, putting homes in that area at a heightened risk of damage. While every residence can weather a 10-year storm without dike protection, the situation turns dire with increased storm severity. Our analysis showed there are homes that cannot stand against a 100-year storm, even with dike protection, especially when factoring in the looming threat of rising sea levels. Under these circumstances, less than 0.5% of homes face submersion. However, it is vital to note that our assessment, which relies on doors on the first floors of buildings, offers just a snapshot of the potential flood damage. Floods can impact other architectural aspects, such as facades, varied openings like windows or air vents, and even the very foundations based on soil types. Consequently, gauging the efficacy of a dike based solely on this method is insufficient. In scenarios devoid of dike protection, the devastation from a storm mirroring Hurricane Ike's intensity would compromise nearly 200 additional homes. Similarly, a 100-year storm could endanger around 450 more homes. These figures emphasize the dike's indispensable protective role. Absent this barrier, the repercussions from storms of such magnitudes would multiply exponentially. Yet, a 500-year storm presents a grim picture, threatening close to 200 homes, with its effects magnified due to SLR. Fortunately, dike protection helps mitigate this, limiting the damage to only 1–2% of homes. Still, the consequences of SLR cannot be ignored. In the absence of a dike and when factoring in SLR, a 100-year storm might submerge an alarming 35% of homes. The impact of a 500-year storm is even more devastating, potentially inundating 40% of homes. To reiterate, the effectiveness

of extensive infrastructure like a dike cannot be judged using a singular approach. A more holistic methodology is imperative to truly understand its impact and efficiency.

These results inform Galveston-area emergency managers' efforts to address several key challenges that Galveston-focused research has identified across the mitigation, preparedness, response, and recovery phases for storm surge events. For the mitigation phase, there is an urgent need for Texas coastal communities to take a more community-specific approach (Olonilua & Ibitayo, 2014), including by more precisely identifying high risk locations and populations (Shultz & Galea, 2017) so that mitigation plans can be tailored based on individualized risk assessments (Xiao & Peacock, 2014) and buyouts can be targeted most effectively (Atoba et al., 2021). Our visualization helps meet this need by showing a property-level depiction of the likely severity of flood damage under multiple scenarios. For the preparedness phase, maps and visualizations that more accurately show Galveston residents their level of risk is needed to inform appropriate preparedness actions, including evacuation (Chen et al., 2016). Xiao and Peacock (2014) showed that appropriate preparedness actions for Galveston stakeholders are highly location dependent since storm surge flood risk varies considerably across the Island and is the strongest predictor of damage. More accurate visualizations of storm surge of flooding and resulting building damage — such as the visualization developed for this study — are therefore essential in promoting appropriate, stakeholder-specific disaster preparedness. For the response phase, research on rescue efforts during the last two major Galveston-area flood events (Ike and Harvey) has highlighted technological solutions to obtaining more precise information on the locations of those in greatest need of assistance during disaster, including via ad hoc wireless networks (George et al., 2010), Twitter posts (Mihunov et al., 2020), and analysis of satellite imagery (Cao & Choe, 2020). Our visualization complements these other technological solutions by helping first responders identify the homes most likely to be flooded or damaged under multiple storm scenarios and enabling them to target their rescue efforts accordingly. Finally, for the recovery phase, Dunning (2020) found that participatory, multi-stakeholder disaster simulation exercises are needed to plan recovery efforts that are more responsive to the needs of the Galveston community. Because our visualization provides a detailed, location specific view of likely flood impacts at the household level, it could help improve such simulation exercises by providing damage estimates that are directly relevant to the interests of many Galveston-area stakeholders.

Our work is also responsive to calls to give more in-depth consideration to the benefits and impacts of actually building and implementing the Ike Dike to protect the concentration of people and property around Galveston Bay (Merrell et al., 2010). As our visualization demonstrates, Galveston has a complex flood hazardscape, with lower vulnerability in elevated areas near the seawall on the east end of the island and higher vulnerability on the bay side and west end. Consistent with earlier visualizations of Galveston flood scenarios with and without the Ike Dike (Retchless et al., 2021), our visualization shows that the Dike is likely to significantly reduce storm surge flooding – and associated property damage – in most areas of the island and for multiple storm surge and sea level rise scenarios. This could be especially beneficial to homes and businesses in low lying areas away from the sea wall that are currently at high risk of flooding during storm surge events without the protection of the Dike.

Future work should expand the scope of our visualization, both thematically (e.g., to include types of structures other than homes, such as businesses) and geographically (to include other coastal communities). Many of the benefits identified for our visualization could extend to other low-lying coastal communities with a significant risk of storm surge flooding. The Galveston area has some of the fastest rates of sea level rise and coastal erosion observed in the U.S. (Luijendijk et al., 2018), but trends show that coastal flooding is also increasing for most U.S. coastal communities, albeit at a slower rate (Sweet et al., 2017). Galveston, therefore, serves as an excellent testbed for tools such as our flood visualization that may soon be urgently needed in many coastal communities. As we have shown for Galveston, similar visualizations could be used in other coastal communities with high flood vulnerability to meet their need for realistic, building-level depictions of flood impacts under multiple storm scenarios, with benefits across the mitigation, preparedness, response, and recovery phases of the disaster management cycle.

We visualize the spread of floods in the 3D view in Galveston, a coastal Texas community. Hence, the users can feel the impact of urban disasters more intuitively. We observe how the flooding spread through different perspectives, and for each house we analyze the damage situation. This animation is not only a visual artifact, but it can also reflect the dynamics of urban disasters and assess the city's resilience to them. Visualization using 3D modeling is the basis for smart cities and urban digital twins (Ye et al., 2021). As we use more methods to evaluate urban disasters, we hope to visualize and query urban disaster information in ways that provide increasingly useful decision support for emergency management and planning (Ye & Niyogi, 2022).

#### Acknowledgements

We thank very much for the valuable comments from anonymous reviewers.

#### Authors' contributions

Conceptualization: Xinyue Ye, Shoujia Li, Ge Gao; Writing—original draft preparation: Xinyue Ye, Shoujia Li, Ge Gao; Writing—review and editing: David Retchless, Zhehang Cai, Galen Newman, Jiaxin Du, Nick Duffield. All authors read and approved the final manuscript.

#### Funding

This material is partially based upon work supported by the National Science Foundation under Grant Nos. 2122054 and 2232533, the start-up Grant 241117–40000 from Texas A&M University's Department of Landscape Architecture and Urban Planning, and the data science course development grant 241123–92000 from Texas A&M Institute of Data Science. Any opinions, findings, and conclusions or recommendations expressed in this material are those of the author and do not necessarily reflect the views of the National Science Foundation and Texas A&M University.

#### Availability of data and materials

The data that support the findings of this study are available the authors upon reasonable request.

#### Declarations

#### Ethics approval and consent to participate

Not applicable.

#### Consent for publication

Yes.

#### Competing interests

The authors declare they have no financial interests.

Received: 29 October 2023 Revised: 10 February 2024 Accepted: 12 February 2024

Published online: 08 May 2024

#### References

- Aditya, T., Iswanto, F., Wirawan, A., & Laksono, D. P. (2011). *3D cadastre web map: Prospects and developments*.
- Atoba, K., Newman, G., Brody, S., Highfield, W., Kim, Y., & Juan, A. (2021). Buy them out before they are built: Evaluating the proactive acquisition of vacant land in flood-prone areas. *Environmental Conservation*, 48(2), 118–126.
- Biljecki, F., Stoter, J., Ledoux, H., Zlatanova, S., & Çöltekin, A. (2015). Applications of 3D city models: State of the art review. *ISPRS International Journal of Geo-Information*, 4(4), 2842–2889.
- Buyukdemircioglu, M., & Kocaman, S. (2020). Reconstruction and efficient visualization of heterogeneous 3D city models. *Remote Sensing*, 12(13), 2128.
- Cai, Z., Newman, G., Lee, J., Ye, X., Retchless, D., Zou, L., & Ham, Y. (2023). Simulating the spatial impacts of a coastal barrier in Galveston Island, Texas: A three-dimensional urban modeling approach. *Geomatics, Natural Hazards and Risk*, 14(1), 2192332. <https://doi.org/10.1080/19475705.2023.2192332>
- Cao, Q. D., & Choe, Y. (2020). Building damage annotation on post-hurricane satellite imagery based on convolutional neural networks. *Natural Hazards*, 103(3), 3357–3376.
- Chang, L.-F., Lin, C.-H., & Su, M.-D. (2008). Application of geographic weighted regression to establish flood-damage functions reflecting spatial variation. *Water Sa*, 34(2), 209–216.
- Chen, Y.-H., Zick, S. E., & Benjamin, A. R. (2016). A comprehensive cartographic approach to evacuation map creation for Hurricane Ike in Galveston County, Texas. *Cartography and Geographic Information Science*, 43(1), 68–85.
- DCMCPartners. (2022). *City of Galveston hazard mitigation plan*.
- De Santis, R., Macchione, F., Costabile, P., & Costanzo, C. (2019). Visual Risk Communication of Urban Flooding in 3D Environments Based on Terrestrial Laser Scanning. In *New Trends in Urban Drainage Modelling: UDM 2018 11* (pp. 783–787). Springer International Publishing.

- Diaz, N. D., Highfield, W. E., Brody, S. D., & Fortenberry, B. R. (2022). Deriving first floor elevations within residential communities located in Galveston using UAS based data. *Drones*, 6(4), 81.
- Douglas, E. (2022). U.S. House approves massive \$31 billion "Ike Dike" project to protect Texas coast from hurricanes. <https://www.texastribune.org/2022/06/09/texas-ike-dike-hurricanes-house-vote/>
- Dübel, S., Röhligh, M., Schumann, H., & Trapp, M. (2014). 2D and 3D presentation of spatial data: A systematic review. In *2014 IEEE VIS international workshop on 3DVis (3DVis)*
- Dunning, K. H. (2020). Building resilience to natural hazards through coastal governance: A case study of Hurricane Harvey recovery in Gulf of Mexico communities. *Ecological Economics*, 176, 106759.
- Gallegos, H. A., Schubert, J. E., & Sanders, B. F. (2009). Two-dimensional, high-resolution modeling of urban dam-break flooding: A case study of Baldwin Hills, California. *Advances in Water Resources*, 32(8), 1323–1335.
- Gallien, T. W., Kalligeris, N., Delisle, M.-P.C., Tang, B.-X., Lucey, J. T., & Winters, M. A. (2018). Coastal flood modeling challenges in defended urban backshores. *Geosciences*, 8(12), 450.
- George, S. M., Zhou, W., Chenji, H., Won, M., Lee, Y. O., Pazarloglou, A., Stoleru, R., & Barooah, P. (2010). DistressNet: A wireless ad hoc and sensor network architecture for situation management in disaster response. *IEEE Communications Magazine*, 48(3), 128–136.
- Lee, Y. Y., Park, H. J., & Oh, S. C. (2019). A Study on the Development of Urban Internal Waters Flooding Visualization System Using Unreal Engine. In *Proceedings of the 40th Asian Conference on Remote Sensing, Daejeon, Republic of Korea* (pp. 14–18)
- Luijendijk, A., Hagenaars, G., Ranasinghe, R., Baart, F., Donchyts, G., & Aarninkhof, S. (2018). The state of the world's beaches. *Scientific Reports*, 8(1), 1–11.
- Marcy, D., Brooks, W., Draganov, K., Hadley, B., Haynes, C., Herold, N., McCombs, J., Pendleton, M., Ryan, S., & Schmid, K. (2011). New mapping tool and techniques for visualizing sea level rise and coastal flooding impacts. In *Solutions to coastal disasters 2011* (pp. 474–490).
- Martínez-Gomariz, E., Forero-Ortiz, E., Russo, B., Locatelli, L., Guerrero-Hidalga, M., Yubero, D., & Castan, S. (2021). A novel expert opinion-based approach to compute estimations of flood damage to property in dense urban environments. Barcelona case study. *Journal of Hydrology*, 598, 126244.
- Marvi, M. T. (2020). A review of flood damage analysis for a building structure and contents. *Natural Hazards*, 102(3), 967–995.
- Merrell, W. J., Reynolds, L. G., Cardenas, A., Gunn, J. R., & Hufton, A. J. (2010). The Ike dike: A coastal barrier protecting the Houston/Galveston region from hurricane storm surge. In *Macro-engineering seawater in unique environments* (pp. 691–716). Springer.
- Merrell, W. J., Reynolds, L. G., Cardenas, A., Gunn, J. R., & Hufton, A. J. (2011). The Ike dike: a coastal barrier protecting the Houston/Galveston region from hurricane storm surge. In *Macro-engineering seawater in unique environments: Arid lowlands and water bodies rehabilitation* (pp. 691–716). Springer.
- Merz, B., Kreibich, H., Schwarze, R., & Thieken, A. (2010). Review article "Assessment of economic flood damage." *Natural Hazards and Earth System Sciences*, 10(8), 1697–1724.
- Mignot, E., Li, X., & Dewals, B. (2019). Experimental modelling of urban flooding: A review. *Journal of Hydrology*, 568, 334–342.
- Mihunov, V. V., Lam, N. S. N., Zou, L., Wang, Z., & Wang, K. (2020). Use of Twitter in disaster rescue: Lessons learned from Hurricane Harvey. *International Journal of Digital Earth*, 13(12), 1454–1466.
- Neal, J., Fewtrell, T., & Trigg, M. (2009). Parallelisation of storage cell flood models using OpenMP. *Environmental Modelling & Software*, 24(7), 872–877.
- Needham, H., & McIntyre, N. (2018). *Analyzing the vulnerability of buildings to coastal flooding in Galveston, Texas*.
- Ning, H., Li, Z., Ye, X., Wang, S., Wang, W., & Huang, X. (2022). Exploring the vertical dimension of street view image based on deep learning: A case study on lowest floor elevation estimation. *International Journal of Geographical Information Science*, 36(7), 1317–1342.
- Notaro, V., De Marchis, M., Fontanazza, C., La Loggia, G., Puleo, V., & Freni, G. (2014). The effect of damage functions on urban flood damage appraisal. *Procedia Engineering*, 70, 1251–1260.
- Olonilua, O., & Ibitayo, O. (2014). An in-depth analysis of the Houston-Galveston Area Council regional hazard mitigation plan under the Disaster Mitigation Act of 2000 (DMA2K). *Risk, Hazards & Crisis in Public Policy*, 5(3), 316–341.
- Ozdemir, H., Sampson, C. C., de Almeida, G. A., & Bates, P. D. (2013). Evaluating scale and roughness effects in urban flood modelling using terrestrial LIDAR data. *Hydrology and Earth System Sciences*, 17(10), 4015–4030.
- Poulter, B., & Halpin, P. N. (2008). Raster modelling of coastal flooding from sea-level rise. *International Journal of Geographical Information Science*, 22(2), 167–182.
- Retchless, D., Mobley, W., Davlasheridze, M., Atoba, K., Ross, A. D., & Highfield, W. (2021). Mapping cross-scale economic impacts of storm surge events: Considerations for design and user testing. *Journal of Maps*, 17(1), 123–135.
- Reyes, M. E. P., & Chen, S.-C. (2017). A 3D virtual environment for storm surge flooding animation. In *2017 IEEE Third International Conference on Multimedia Big Data (BigMM)*.
- Romali, N. S., Yusop, Z., Sulaiman, M., & Ismail, Z. (2018). Flood risk assessment: A review of flood damage estimation model for Malaysia. *Jurnal Teknologi*, 80(3), 145–153.
- Sanders, B. F. (2007). Evaluation of on-line DEMs for flood inundation modeling. *Advances in Water Resources*, 30(8), 1831–1843.
- Schinke, R., Kaidel, A., Golz, S., Naumann, T., López-Gutiérrez, J. S., & Garvin, S. (2016). Analysing the effects of flood-resilience technologies in urban areas using a synthetic model approach. *ISPRS International Journal of Geo-Information*, 5(11), 202.
- Shojaei, D., Kalantari, M., Bishop, I. D., Rajabifard, A., & Aien, A. (2013). Visualization requirements for 3D cadastral systems. *Computers, Environment and Urban Systems*, 41, 39–54.
- Shultz, J. M., & Galea, S. (2017). Preparing for the next Harvey, Irma, or Maria—Addressing research gaps. *New England Journal of Medicine*, 377(19), 1804–1806.
- Smith, D. I. (1994). Flood damage estimation—A review of urban stage-damage curves and loss functions. *Water Sa*, 20(3), 231–238.
- Smith, K., & Ward, R. C. (1998). *Floods: Physical processes and human impacts. (No Title)*.
- Souza, L., & Bueno, C. (2022). City Information Modelling as a support decision tool for planning and management of cities: A systematic literature review and bibliometric analysis. *Building and Environment*, 207, 108403.
- Sweet, W. V., Kopp, R. E., Weaver, C. P., Obeysekera, J., Horton, R. M., Thieler, E. R., & Zervas, C. (2017). *Global and regional sea level rise scenarios for the United States*.
- Wang, C.-Y., Liao, H.-Y.M., Wu, Y.-H., Chen, P.-Y., Hsieh, J.-W., & Yeh, I. H. (2020). *CSPNet: A new backbone that can enhance learning capability of CNN* (pp. 390–391)
- Wu, W., Liu, H., Li, L., Long, Y., Wang, X., Wang, Z., Li, J., & Chang, Y. (2021). Application of local fully Convolutional Neural Network combined with YOLO v5 algorithm in small target detection of remote sensing image. *PLoS One*, 16(10), e0259283.
- Xiao, Y., & Peacock, W. G. (2014). Do hazard mitigation and preparedness reduce physical damage to businesses in disasters? Critical role of business disaster planning. *Natural Hazards Review*, 15(3), 04014007.
- Ye, X., Du, J., Han, Y., Newman, G., Retchless, D., Zou, L., Ham, Y., & Cai, Z. (2023). Developing human-centered urban digital twins for community infrastructure resilience: A research agenda. *Journal of Planning Literature*, 38(2), 187–199.
- Ye, X., & Niyogi, D. (2022). Resilience of human settlements to climate change needs the convergence of urban planning and urban climate science. *Computational Urban Science*, 2(1), 1–4.
- Ye, X., Wang, S., Lu, Z., Song, Y., & Yu, S. (2021). Towards an AI-driven framework for multi-scale urban flood resilience planning and design. *Computational Urban Science*, 1(1), 1–12.
- Zabret, K., Hozjan, U., Kryžanowsky, A., Brilly, M., & Vidmar, A. (2018). Development of model for the estimation of direct flood damage including the movable property. *Journal of Flood Risk Management*, 11, S527–S540.
- Zhang, T., Feng, P., Maksimović, Č., & Bates, P. D. (2016). Application of a three-dimensional unstructured-mesh finite-element flooding model and comparison with two-dimensional approaches. *Water resources management*, 30, 823–841.

## Publisher's Note

Springer Nature remains neutral with regard to jurisdictional claims in published maps and institutional affiliations.